Biochimica et Biophysica Acta 1838 (2014) 2105–2114

Contents lists available at ScienceDirect

Biochimica et Biophysica Acta

journal homepage: www.elsevier.com/locate/bbamem

L_o/L_d phase coexistence modulation induced by GM1

Nicolas Puff [a,b,*], Chiho Watanabe [b], Michel Seigneuret [b], Miglena I. Angelova [a,b], Galya Staneva [c]

[a] UPMC Univ. Paris 06, UFR 925 Physics Department, Paris, France
[b] Laboratoire Matière et Systèmes Complexes (MSC), UMR 7057 CNRS and Université Paris Diderot—Paris 7, Paris, France
[c] Institute of Biophysics and Biomedical Engineering, Bulgarian Academy of Sciences, Sofia, Bulgaria

ARTICLE INFO

Article history:
Received 29 October 2013
Received in revised form 30 April 2014
Accepted 3 May 2014
Available online 13 May 2014

Keywords:
GM1
GUV
Laurdan
Microdomain
Nanoscale domain
L_o/L_d phase coexistence

ABSTRACT

Lipid rafts are assumed to undergo biologically important size-modulations from nanorafts to microrafts. Due to the complexity of cellular membranes, model systems become important tools, especially for the investigation of the factors affecting "raft-like" L_o domain size and the search for L_o nanodomains as precursors in L_o microdomain formation. Because lipid compositional change is the primary mechanism by which a cell can alter membrane phase behavior, we studied the effect of the ganglioside GM1 concentration on the L_o/L_d lateral phase separation in PC/SM/Chol/GM1 bilayers. GM1 above 1 mol % abolishes the formation of the micrometer-scale L_o domains observed in GUVs. However, the apparently homogeneous phase observed in optical microscopy corresponds in fact, within a certain temperature range, to a L_o/L_d lateral phase separation taking place below the optical resolution. This nanoscale phase separation is revealed by fluorescence spectroscopy, including C_{12}NBD-PC self-quenching and Laurdan GP measurements, and is supported by Gaussian spectral decomposition analysis. The temperature of formation of nanoscale L_o phase domains over an L_d phase is determined, and is shifted to higher values when the GM1 content increases. A "morphological" phase diagram could be made, and it displays three regions corresponding respectively to L_o/L_d micrometric phase separation, L_o/L_d nanometric phase separation, and a homogeneous L_d phase. We therefore show that a lipid only-based mechanism is able to control the existence and the sizes of phase-separated membrane domains. GM1 could act on the line tension, "arresting" domain growth and thereby stabilizing L_o nanodomains.

© 2014 Elsevier B.V. All rights reserved.

1. Introduction

Cell plasma membrane contains hundreds of lipids and proteins designed to perform the functions that cells require. It is now established that these membranes are mosaics of different types of domains with different sizes, compositions, dynamics and functions [1,2]. Among the various types of membrane domains, several are based on lipid interactions, with the most documented being the so-called lipid rafts [3,4]. These appear to be involved in many biological functions involving cellular activation, membrane trafficking, and signal transduction.

Rafts are thought to be rich in sphingolipids, cholesterol, and specific proteins [5,6] with lipids that are in a phase state that is distinct from the surrounding membrane [7]. Indeed, it is often speculated that this raft organization arises from the tendency for lipids in membranes containing cholesterol to separate into coexisting liquid-ordered (L_o) and liquid-disordered (L_d) phases [8,9]. The raft hypothesis elevated lipids to a regulatory role in which they mediate protein clustering and restrict protein diffusion in the membrane [4]. While the key role of cholesterol and sphingolipids is clear, this definition implies long-lived structures with stable protein recruitment. However, because the characterization of these membrane heterogeneities in live cells has been challenged, the idea of what constitutes a lipid raft has evolved. Indeed, large-scale membrane domains are not optically observable without significant perturbation [10,11] and the biochemical methodology used to study rafts has generated ambiguous results [12,13]. Currently, lipids rafts are viewed as highly dynamic nanoscale assemblies [14,15] that could undergo coalescence into micrometer-sized domains during specific cellular activation process [16,17]. This feature may be pivotal to the raft function and raft size is of crucial importance in the study of cellular functioning.

Abbreviations: L_o, liquid-ordered phase; L_d, liquid-disordered phase; GUV, giant unilamellar vesicle; Chol, cholesterol; GPMV, giant plasma membrane vesicle; DSPC, distearoyl-phosphatidylcholine; DOPC, dioleolyl- phosphatidylcholine; POPC, 1-palmitoyl-2-oleoyl-sn-glycero-3-phosphocholine; GM1, ovine brain monosialotetrahexosylganglioside; PC, egg yolk L-α-phosphatidylcholine; SM, egg yolk sphingomyelin; Laurdan, 6-dodecanoyl-2- dimethylaminonaphthalene; C_{12}NBD-PC, 1-acyl-2-[12-[(7-nitrobenz-2-oxa-1,3-diazol-4-yl)amino]dodecanoyl]-sn-glycero-3-phosphocholine; TR-PE, Texas red DPPE; GP, generalized polarization; LUV, large unilamellar vesicle; T_{IP}, temperature at the inflection point

* Corresponding author at: Laboratoire Matière et Systèmes Complexes (MSC), CNRS UMR 7057, Université Paris Diderot—Paris 7, Bât. Condorcet, case 7056, 10, rue Alice Domon et Léonie Duquet, 75205 Paris Cedex 13, France. Tél.: +33 1 57 27 70 82; fax: +33 1 57 27 62 11.
E-mail address: nicolas.puff@univ-paris-diderot.fr (N. Puff).

http://dx.doi.org/10.1016/j.bbamem.2014.05.002
0005-2736/© 2014 Elsevier B.V. All rights reserved.

In contrast to in vivo membranes, L_o/L_d phase separation in model membranes can easily be induced by adjusting the composition and temperatures of lipid bilayers. In particular, giant unilamellar vesicles (GUVs) allow optical fluorescence discrimination of coexisting lipid phases. Using simple biologically relevant lipid model systems composed of a high transition temperature (T_m) lipid, a low-T_m lipid, and cholesterol (Chol), micron-scale domains (raft-like or L_o microdomains) have been observed on GUVs [9,18], and are believed to represent the in vitro equivalent of the rafts in natural membranes. The usual approach for studying the formation of L_o microdomains in GUVs is to use a range of lipid compositions for their preparation and/or to vary the temperature. These studies have yielded important results, culminating in the determination of several L_o/L_d phase diagrams for specific lipid mixtures [19,20]. GUVs containing L_o microdomains coexisting with an L_d phase, have become important tools for the modeling of properties and biological functions of lipid rafts [19,20]. These have been also instrumental in evaluating current ideas as well as making new proposals for raft-associated mechanisms [21–23].

However, the biological relevance of L_o microdomains on GUVs systems has been questioned because, in comparison to in vivo membranes, such domains are stable equilibrium structures with a larger micrometric size. First, it has to be noticed that the use of techniques other than optical microscopy to probe shorter length scales that are biologically relevant provides evidence for much smaller L_o domains [24–26], even with lipid mixtures and temperatures for which fluorescence microscopy indicates only the presence of a single homogeneous phase [27]. On the other hand, it has been shown that giant plasma membrane vesicles (GPMVs, same membrane composition as intact cells but lacking a cytoskeleton) formed from the plasma membranes of cultured mammalian cells can segregate in micrometer-scale fluid domains [28,29]. Coexisting fluid membrane phases in GPMVs show fluorescence probe partitioning behavior similar to model membranes with L_o/L_d phase coexistence. As emphasized by Hancock [30], "there is no a priori reason to assume that the basic lipid biochemistry and thermodynamics that operate in model systems are not the same as those that operate in the plasma membrane", and a systematic study of the factors affecting domain size is clearly needed.

Recent work from Feigenson et al. [31,32] has investigated a domain size transition in the four-component mixture DSPC/DOPC/POPC/Chol, which may yield insight into how cells are able to exploit lipid composition changes to alter the size and connectivity of domains. These studies establish that both the size and morphology of membrane L_o domains can be controlled by the concentration and the type of low-melting lipid in mixtures of cholesterol and high-melting lipid. Another fourth appropriate candidate to add to the classical raft-like-domain-making three component lipid mixtures could be the ganglioside GM1. Indeed, gangliosides are known as major players in the creation of lateral order within biological membranes [33]. They are essential components of rafts and are directly involved in several raft-associated cellular processes [34]. GM1 has a strong amphiphilic character due to the big saccharidic headgroup that bears a protonatable sialic acid moiety, and the saturated double-tailed hydrophobic moiety. GM1 can separate from unsaturated lipids as a result of immiscibility [35] and seems to be preferentially distributed in the L_o domains in model systems [36,37]. Moreover, because of the excluded volume effect of its bulky headgroup, GM1 can also segregate from other saturated lipids and be heterogeneously distributed in submicron-sized domains within the ordered phase [38]. Concerning the domain size modulation, AFM experiments show that asymmetrically-inserted GM1 on pre-formed supported lipid bilayers promotes not only a change in the dominant lipid component of the L_o phase but also, a decrease of the L_o domain area with increasing GM1 concentration [39]. These complex intermolecular interactions between GM1 and saturated lipids, unsaturated lipids, and cholesterol, allow the membrane structure to be modulated with an incredible diversity via distinct mechanisms. Because each method introduces a different set of issues and the same set of lipid mixtures are rarely used, further experiments on four-component mixtures containing GM1 are still needed to improve the role of GM1 on L_o domain size modulation.

In the present work, the effect of GM1 concentration on the lateral phase separation in the PC/SM/Chol (50:30:20) bilayers was studied by fluorescence microscopy and spectroscopy. As expected for this lipid mixture below 23 °C without GM1 [40], fluorescence microscopy shows the occurrence of micrometer-sized L_o domains in GUVs. Oppositely, GUVs displaying a homogeneous phase are observed at higher temperature. Interestingly, GM1 above 1 mol % abolishes the formation of micrometer-scale L_o domains. We show however that the homogeneous phase observed in that case by optical microscopy corresponds in fact, for a certain temperature range, to a L_o/L_d lateral phase separation below the optical resolution. This nanoscale phase separation is revealed by fluorescence spectroscopy on LUVs, including of C_{12}NBD-PC self-quenching and Laurdan GP measurements, and is supported by Gaussian spectral decomposition analysis. This allowed us to determine the temperature of formation of L_o phase domains over an L_d phase. The determined demixing temperatures from L_d to L_o/L_d phase separation are shifted to higher values when the GM1 content increases, which is linked with the change of the dominant composition of L_o domains. A lipid only-based mechanism is consequently able to control the existence and the sizes of phase-separated membrane domains. This last feature is tentatively attributed to GM1 effect on the line tension, "arresting" domain growth and thereby stabilizing L_o nanodomains.

2. Materials and methods

2.1. Reagents

Lipids were obtained as follows and used without further purification: egg yolk L-α-phosphatidylcholine (PC), egg yolk sphingomyelin (SM), cholesterol (Chol) and ovine brain GM1 were from Avanti Polar Lipids. The fluorescent lipid analogue Texas red DPPE (TR-PE) was from Invitrogen and the lipophilic membrane probe C_{12}NBD-PC (1-acyl-2-[12-[(7-nitrobenz-2-oxa-1,3-diazol-4-yl)amino]dodecanoyl]-sn-glycero-3-phosphocholine) was obtained from Avanti Polar Lipids. Fluorescent probe 6-dodecanoyl-2- dimethylaminonaphthalene (Laurdan) was from Molecular Probes, Inc. All others chemicals were of highest purity grade.

2.2. Giant unilamellar vesicle preparation and imaging

The electroformation method developed by Angelova and Dimitrov [41] was used to form the vesicles. We followed the particular protocol for giant unilamellar heterogeneous vesicle formation described elsewhere [42]. GUVs were prepared with the starting molar composition PC/SM/Chol 50:30:20. GM1 was substituted for SM in proportions from 1 to 10 mol %. The vesicles were formed in a temperature-controlled chamber in 0.5 mM HEPES buffer, pH 7.4. The temperature was controlled with a water circulating bath. The vesicles were always formed at 45 °C at which a high yield of vesicles was consistently obtained. Texas red phosphatidylethanolamine (TR-PE) was used as a probe at a concentration of 0.25% (mol/mol). TR-PE partitions in favor of the L_d phase [9] which appears brighter while the L_o phase appears darker by fluorescence microscopy.

A Zeiss Axiovert 200M microscope (fluorescent unit fluo arc N HBO 103, Zeiss), equipped with a Lambda 10-2 unit (Sutter Instrument Co.), plus a CCD B/W chilled camera (CoolSNAP HQ, Photometrics) was used for GUV imaging. The setup was computer-controlled by the Metamorph 6.2 software (Molecular Devices). A 40× Ph LD Zeiss objective was used. The phase morphology transformations and dynamics in the heterogeneous GUV membranes were followed by fluorescence using Zeiss filter set 15 (E_x/E_m = 550/620 nm).

2.3. Large unilamellar vesicle preparation and spectroscopic fluorescence measurements

Large unilamellar vesicles (LUVs) were prepared using the extrusion method [43] in HEPES 5 mM, pH 7.4, EDTA 0.1 mM as described previously [44]. Samples were prepared by dissolving and mixing the indicated lipids in chloroform/methanol (9.4:0.6 *v*/*v*) to obtain the desired compositions. In the self-quenching experiments, C_{12}NBD-PC concentration was 4 mol %. The fluorescent probe Laurdan was mixed with the lipids in the initial organic solution at a Laurdan:lipid ratio of 1:200. LUV samples were kept at 4 °C, and used for measurements the day after.

Steady-state fluorescence measurements were carried out with a Cary Eclipse spectrofluorimeter (Varian Instruments, CA) equipped with a thermostated cuvette holder (±0.1 °C). Quartz cuvettes were used. Excitation and emission slits were adjusted to 5 nm. All fluorescence measurements were carried out at a total lipid concentration of 0.5 mM for C_{12}NBD-PC self-quenching experiments, and 0.2 mM for Laurdan measurements. Cooling temperature scans were performed with several measurements from 60 to 10 °C, allowing sample equilibration for 5 min when the desired temperature is reached. We checked (i) that there was no hysteresis when the temperature scan was done heating the sample from 10 to 60 °C, and (ii) that the probe emission was stable with time after a 5 min incubation, indicating that the system has reached the steady-state.

We monitored the L_o/L_d phase coexistence through the concentration-dependent self-quenching of C_{12}NBD-PC known to be mostly excluded from the L_o phase [45]. C_{12}NBD-PC fluorescence was excited at 470 nm, and emitted fluorescence maximum was measured at 538 nm.

Laurdan is known to be very sensitive to the phase state of the membrane. The basis of Laurdan spectral sensitivity lies in its ability to sense the polarity and dynamics of dipoles in the immediate environment due to its dipolar relaxation processes. Excitation wavelength for Laurdan was 355 nm. All emission spectra (from 370 to 600 nm) were recorded twice and averaged. Analysis of the steady-state spectra was performed using IGOR 6.10A (WaveMetrics). Polarity changes are shown by shifts in the Laurdan emission spectrum, which are quantified by calculating the generalized polarization (GP) defined as $GP = (I_{440} - I_{490})/(I_{440} + I_{490})$ where I_{440} and I_{490} are the emission intensities at 440 and 490 nm respectively [46]. GP values can theoretically assume values from +1 (being the most ordered) and -1 (being the least ordered). GP measurements are done by simply registering the two mentioned emission intensities (2 sets of 5 measurements averaged).

3. Results

3.1. GM1 concentration effect on the L_o/L_d phase coexistence in GUVs

GUVs were prepared at 45 °C with the starting molar composition PC/SM/Chol 50:30:20. This composition was chosen because it yields L_o microdomains below 23 °C [40]. Texas red phosphatidylethanolamine (TR-PE) was used as a probe. It partitions in favor of the L_d phase [9] which appears brighter while the L_o phase appears darker by fluorescence microscopy. Starting from 45 °C without any prior fluorescence illumination, the temperature was decreased. At a chosen temperature, each specific isolated GUV is illuminated in fluorescence and the presence of a L_o/L_d phase coexistence is checked. This protocol was repeated with several vesicles for different temperatures and allows the phase-separation-temperature to be determined without any artifacts coming from possible light-induced lipid chemical modification [47]. As expected, below 23 °C, fluorescence microscopy of these GUVs shows the occurrence of micrometer-size domains initiated by nucleation. Oppositely, GUVs displaying a homogeneous phase are observed at higher temperature. The same kind of experiment was done with different amounts of GM1, substituted for SM in proportions from 1 to 10 mol %. The presence of GM1 was found to have a profound influence on the GUV's bilayer phase separation. Indeed, while with 1 mol % GM1 the temperature at which L_o microdomains over an L_d phase appears, is just slightly decreased to 20 °C, and no visible phase separation occurs with more than 1 mol % GM1 for any temperature above 15 °C. Fig. 1A summarizes the different results as a function of the GM1 molar ratios and temperature. This "morphological" phase diagram shows therefore only 2 regions: L_o microdomains over an L_d phase corresponds to region I whereas an optically homogeneous phase is associated to region II. Some vesicle images corresponding to representative points near the regions boundary on Fig. 1A are shown in Fig. 1B. Two explanations are possible for the existence of region II with the corresponding lipid mixtures. One is that GM1 at more than 1 mol % intrinsically destabilizes the L_o phase due to weaker interactions with other lipids. While this explanation cannot be excluded, this does not seem in agreement with current comparative thermotropic data on these interactions [48]. Another explanation is that GM1 could "arrest" L_o domain growth. This would therefore stabilize nanoscale L_o domains and thereby hinder (for 1 mol % GM1), even abolish (for higher GM1 concentrations) the formation of L_o microdomains. In this case, the membrane might be in the state of a 2D microemulsion, which is globally homogeneous but locally phase-separated. This trend could be attributed to different physical mechanisms that will be discussed afterwards. Anyway, the use of techniques other than optical microscopy

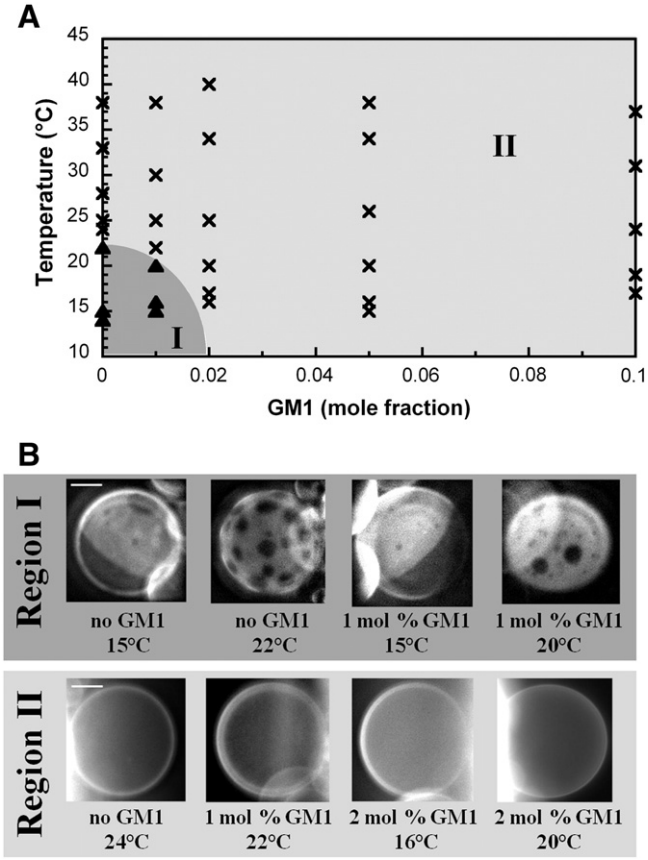

Fig. 1. GM1 concentration effect on the L_o/L_d phase coexistence in GUVs. (A) Phase behavior of PC/SM/Chol/GM1 GUVs as a function of temperature and GM1 mole fraction presented as a morphology diagram. GUVs were prepared with the molar composition PC/SM/Chol/GM1 50:30-*x*:20:*x* ($0 \le x \le 10$) mol/mol. Texas red phosphatidylethanolamine (TR-PE, 0.25 mol %) was used as a probe. Each point corresponds to the evolution of a single GUV, and data are gathered from two or three different samples for each GM1 concentration. Each region represents one type of phase morphology: Region I (▲), L_o microdomains over an L_d phase; region II (x), optically homogeneous phase. (B) Images of GUVs illustrating the effect of temperature and GM1 molar fraction on the L_o/L_d phase coexistence in GUVs. Scale bar = 10 μm.

to probe shorter length scales would provide ample evidence of the existence of L_o nanodomains.

3.2. Evidence of nanoscale L_o/L_d phase coexistence from fluorescence probe self-quenching experiments.

Based on our previous work [45], the concentration self-quenching properties of C_{12}NBD-PC were employed in order to reveal the L_o/L_d phase co-existence. Indeed, it is known that NBD fluorescence intensity in lipid membranes is modulated by two mechanisms: (i) effect of the environment on the NBD fluorescence, i.e., the membrane composition and structure [49,50] as well as by (ii) concentration-dependent NBD self-quenching, i.e., by the concentration of the NBD fluorophore in lipid membrane [51]. In addition, as originally proposed by Hoekstra [52], self-quenching has been recognized as the dominant mechanism for change in the quantum yield of NBD in lipid membranes. An important feature of NBD lipid analogues is their unequal partitioning between the different lipid phases coexisting in a lipid membrane, resulting in the almost complete exclusion of the C_{12}NBD-PC from ordered lipid phases [53]. Consequently, the formation and increase of L_o phase membrane fraction in the vesicles under temperature decreases will lead to a decrease of fluorescence intensity consistent with the exclusion of the fluorescent probe from the L_o phase [45].

Fig. 2 displays the effect of temperature on the relative normalized fluorescence intensity of C_{12}NBD-PC (4 mol %) embedded in different lipid composition bilayers: pure egg PC, in liquid disordered (L_d) phase over the temperature range 10 to 60 °C (T_m around -5 °C, [54]); PC/SM/Chol 46:30:20 (mol/mol), known from our GUV experiments to yield L_o microdomains below 23 °C (Fig. 1A); and PC/SM/Chol/GM1 46:25:20:5 (mol/mol), known from our GUV experiments to be optically homogeneous over the entire temperature range studied (Fig. 1A). With decreasing temperature, the homogeneous bilayer (pure PC) becomes more ordered which is reflected by a monotonic increase of the relative normalized fluorescence intensity as a convex curve (Fig. 2, ○). This order results in lower penetration of water molecules into ordered lipid bilayer, thereby decreasing the polarity in the NBD environment with a consequent increase in NBD fluorescence intensity. If one considers now the curve of C_{12}NBD-PC-containing vesicles having a composition in which there is formation of L_o phase microdomains within a designated range of temperature, i. e. PC/SM/Chol 46:30:20 (mol/mol), the variation of the relative normalized fluorescence intensity with temperature is no longer convex but sigmoidal (Fig. 2, □). Indeed, upon cooling, the relative normalized fluorescence intensity curve presents an inflection followed by a slower increase with increasing temperature, resulting from the self-quenching of the C_{12}NBD-PC accumulated in the remaining membrane fraction in L_d phase. The curve inflection observed here may correspond to the miscibility transition and formation of L_o phase [45]. The inflection is observed at a temperature equal to 28.9 °C. These results (i) confirm the GUV experiments, i.e., the formation and expansion of L_o phase domains within the membrane when the temperature decreases, and (ii) highlight a difference between the temperatures of formation of L_o domains determined with the two different approaches. There is formation of L_o nanodomains at approximately 28.9 °C while L_o microdomains appear at 23 °C. Another striking point is that the curve for the C_{12}NBD-PC-containing vesicles having a composition in which only an optically homogeneous phase is observed over the entire temperature range in our GUV experiments, i.e. PC/SM/Chol/GM1 46:25:20:5 (mol/mol), presents the same sigmoidal fluorescence intensity profile (Fig. 2, ●). This indicates C_{12}NBD-PC self-quenching, i.e., formation of L_o phase domains upon cooling. The lipid-driven lateral separation of immiscible liquid phases (L_d and L_o phases) still takes place at 5 mol % GM1, but within a scale below the optical resolution. Consequently, the "morphological" phase diagram based on our GUV experiments (Fig. 1A) has to be improved with regards to these results.

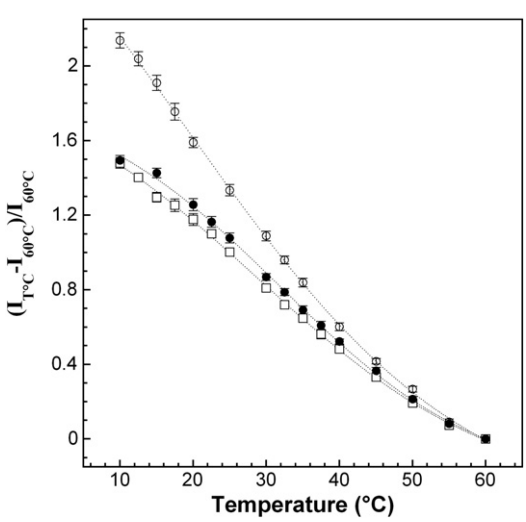

Fig. 2. Temperature dependence of C_{12}NBD-PC relative normalized intensity for 4 mol % C_{12}NBD-PC in LUVs of different compositions. PC (○), PC/SM/Chol/GM1 46:30-x:20:x (mol/mol) with $x = 0$ (□), and $x = 5$ (●). C_{12}NBD-PC fluorescence was excited at 470 nm, and emitted fluorescence maximum was measured at 538 nm. All measurements were carried out at a lipid concentration of 0.5 mM and were recorded at pH 7.4. Sample temperature was gradually decreased. After few minute equilibration under agitation, the measurements were done.

3.3. Determination of the demixing temperature of nanoscopic L_o/L_d phase separation by Laurdan fluorescence.

We then investigated whether the GM1-dependent concentration effect on L_o domain formation could have their counterpart at the molecular level. We therefore studied the effect of GM1 concentration on lipid packing properties using LUVs with Laurdan as a fluorescent probe. Its fluorescence in lipid membranes undergoes a shift in its emission spectrum due to a packing-dependent environmental sensitivity of its excited state relaxation [46]. This is usually expressed as the general polarization GP which is a measure of lipid packing at the molecular level. Laurdan is also believed to show no preferential phase partitioning between ordered and disordered lipid phases and is considered to have uniform lateral and transbilayer distribution [55]. It must be emphasized that considering its spectroscopic properties, Laurdan fluorescence data is expected to yield an essentially static picture of the nanodomain organization. Indeed, the lateral diffusion coefficient of Laurdan is of the same order of magnitude as that of phospholipids, i.e. around $D_T = 5\ \mu m^2\ s^{-1}$, both in L_o and L_d phases [56]. The characteristic time for exchange of Laurdan between L_o nanodomains and L_d phase can be estimated as $L^2/4D_T = 0.5$ ms, $L = 100$ nm being the size range of nanodomains [30]. This is to be compared to the 5 ns fluorescence lifetime of the probe [57]. Therefore, Laurdan spectra correspond to the sum of contributions of probes uniformly [55] distributed between L_o and L_d phases.

3.3.1. Role of GM1 on membrane properties at the molecular level

Fig. 3A displays the effect of GM1 concentration and temperature on Laurdan GP values for LUV lipid compositions similar to those studied with GUVs (PC/SM/Chol/GM1 50:30-x:20:x; $0 \le x \le 10$). As expected, for the overall lipid compositions tested, GP values decrease when the temperature increases. This suggests that at high temperatures, the membrane becomes less packed thereby imparting higher mobility at the membrane interface (where Laurdan is located) which leads to an increase in the dipolar relaxation in this region of the membrane. Moreover, at all temperatures, the increase of the GM1 content from 1 to 10 mol % leads to a GP shift to higher values (Fig. 3A), a feature which can be related to the known ordering effect of GM1[48,58]. It appears from three different AFM studies [36,38,39] that, although GM1 has a

preference for the L_o phase, it can also partition in the L_d phase depending on its average concentration and the specific amount of the other lipid components. Therefore it is reasonable to assume that GM1 is distributed between the two phases (when coexistence occurs) and leads on average to a high membrane order. As a control, we measured the GP temperature dependence for LUV lipid compositions typical of L_d (pure egg PC, [54]) and pure L_o (SM/Chol 50:50 mol/mol, [59]) phases with different GM1 amounts (Fig. 3B and C). As expected, at a given temperature, the GP values are much larger for vesicles in the L_o phase than for those in the L_d phase. Moreover, as for the lipid mixtures designed to exhibit L_o/L_d phase coexistence (Fig. 3A), pure L_d and L_o LUVs present the same GP temperature dependence and the same tendency to higher GP values in the presence of GM1. However, since the L_o phase is already nearly maximally packed, the further increase of packing that can be achieved by GM1 incorporation is limited (Fig. 3C). Oppositely, for the L_d phase which is intrinsically more loosely packed, incorporated GM1 can generate a higher increase in lipid packing (Fig. 3B). The distinct effect of 10 mol % GM1 on the different lipid systems is summarized and further emphasized in Fig. 3D where GP values are plotted as a function of temperature. As expected, GP values for L_o/L_d lipid systems are intermediate between pure L_o and L_d phases and, as mentioned previously, GM1 leads to high membrane order whatever the lipid bilayer composition.

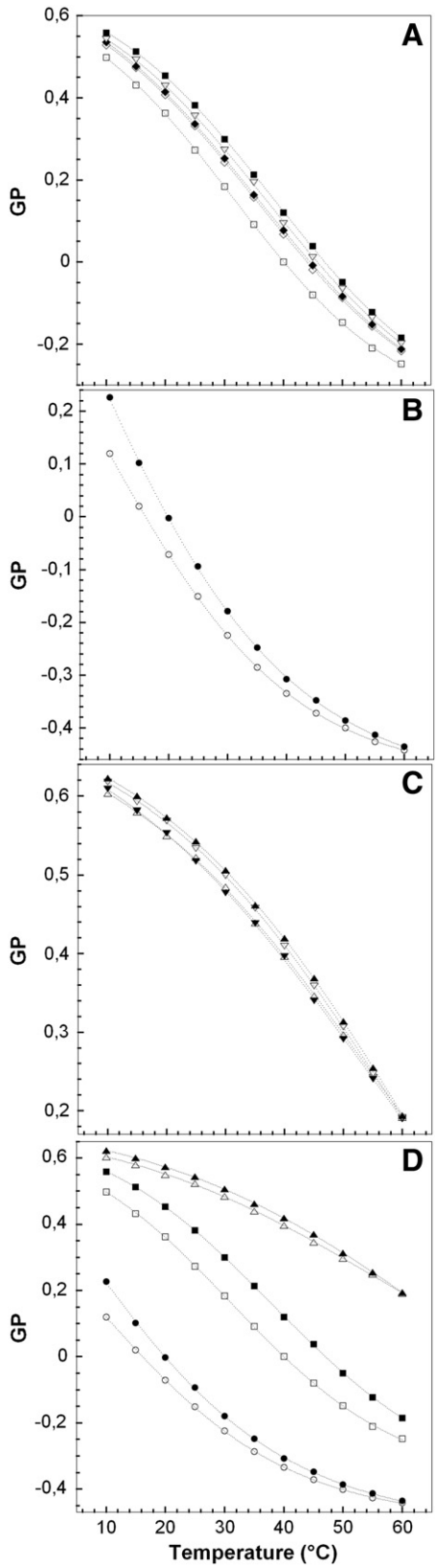

Fig. 3. Effect of temperature and GM1 on lipid packing in LUVs as measured by Laurdan experiments. All measurements were carried out at a lipid concentration of 0.2 mM and were recorded at pH 7.4. Sample temperature was gradually decreased. After few minute equilibration under agitation, the measurements were done. (A) Evolution of GP with temperature for LUVs composed of PC/SM/Chol/GM1 50:30-x:20:x mol/mol with $x = 0$ (□), $x = 1$ (◊), $x = 2$ (◆), $x = 5$ (▽), and $x = 10$ (■). (B) Evolution of GP with temperature for LUVs composed of PC (○), and PC/GM1 90:10 mol/mol (●). (C) Evolution of GP with temperature for LUVs composed of SM/Chol/GM1 50-(x/2):50-(x/2):x mol/mol with $x = 0$ (△), $x = 1$(▼), $x = 5$ (▽), and $x = 10$ (▲). (D) Evolution of GP with temperature for LUVs composed of SM/Chol 50:50 mol/mol (△), SM/Chol/GM1 45:45:10 mol/mol (▲), PC/SM/Chol 50:30:20 mol/mol (□), PC/SM/Chol/GM1 50:20:20:10 mol/mol (■), PC (○), and PC/GM1 90:10 mol/mol (●). The lines are added only to guide the eye.

3.3.2. Sigmoid-like shape of the GP temperature dependence for lipid mixtures designed to exhibit L_o/L_d phase coexistence

The GP values measured in bulk lipid correspond to the sum of the different relative contributions existing in the sample (see above). Nevertheless, several points pertaining to bilayer heterogeneity can be highlighted with a deeper investigation of the plots displayed in Fig. 3. First, a gradual change of membrane order as a function of temperature is observed for all the lipid mixtures. Secondly, the plots for pure L_d and L_o LUVs – and for these LUV compositions with an increasing amounts of GM1 – present a GP decrease with increasing temperature displaying a single concavity (convex for L_d LUVs, Fig. 3B; concave for L_o LUVs, Fig. 3C). On the other hand, L_o/L_d lipid system plots have a sigmoid-like shape with an inflection point, and this feature remains whatever the GM1 content in the membrane (Fig. 3A).The persistence of such a curve-shape above 1 mol % GM1 is another indication for L_o/L_d phase separation at the nanoscale for high GM1 content. Indeed, in agreement with NBD quenching data, the concave to convex transition seen in all curves in Fig. 3A corresponds to the appearance of the L_o/L_d phase coexistence. Such data allows the determination of a demixing temperature range for L_o/L_d phase separation. So, we fitted the data of change in GP with temperature to a sigmoid regression function to derive a value for the temperature at the inflection point (T_{IP}). This temperature represents an approximate (due to the inherent limitations of such curve fitting) demixing temperature. As an example, Fig. S1 (Supporting Information) displays for one lipid mixture (PC/SM/Chol 50:30:20 mol/mol) the GP evolution as a function of temperature, its sigmoid fit, and the sigmoid function derivative. Here, the value of the T_{IP} is equal to 31.4 °C (this value, determined with the fit, corresponds to the minimum of the derivative function, which is shown for more clarity). The same fitting procedure is then applied to all curves presented in Fig. 3A, and the result is that the higher the GM1 content, the higher the T_{IP} is (Fig. 4) (it should be emphasized that in spite of the possible uncertainty on T_{IP} determination, this variation is significant since it can already be inferred from the raw data of Fig. 3A). This last feature is consistent with the fact that increasing GM1 mole fraction leads to

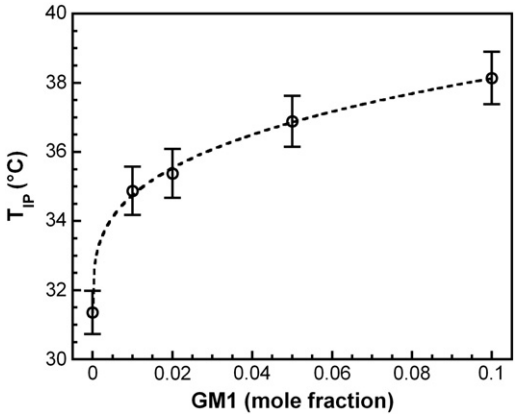

Fig. 4. Evolution with GM1 mole fraction of the temperature (T_{IP}) at the inflection point of sigmoid-like GP curves. T_{IP} values (○) for LUVs composed of PC/SM/Chol/GM1 50:30-*x*:20:*x* mol/mol ($0 \leq x \leq 10$). The line is added only to guide the eye.

the change in the dominant lipid component of the L_o phase from SM to SM/GM1 [39], and consequently to the T_{IP} value.

3.4. Gaussian decomposition analysis of the Laurdan emission spectra

One of the limitations of the experiments presented in Fig. 3 is the measurement of an average or bulk parameter, GP, that samples the bilayer as a whole. Fig. S2 displays Laurdan emission spectra recorded at different temperatures ranging from 10 to 60 °C for LUVs made of PC/SM/Chol 50:30:20 (mol/mol). As expected when the temperature increases, there is a shift of the spectral maximum to higher wavelength. The peak at 490 nm becomes more pronounced, i.e., the GP values decrease (Fig. 3A; (□), 0 mol % GM1).

In order to get more detailed information on the bilayer structural changes, we have attempted to decompose the experimentally obtained emission spectra into simple Gaussian components. Indeed, it was shown that the analysis of the spectral decomposition of the Laurdan emission spectrum is more sensitive to bilayer structural changes than the GP, and that the spectral decomposition has to be done as a function of energy, and not the wavelength [60]. This kind of two- or three-Gaussian component decomposition has been already carried out in previous analyses of Laurdan fluorescence spectra in model [60,61] and biological membranes [62], and could be informative in view of the ability of Laurdan to be excited to and to emit from different states in an environment-dependent-manner. This sensitivity originates mainly upon the probe interaction with surrounding water during its 5 ns excited state. Hydrogen bonding, as well as the relaxation of water molecules which maximizes dipole–dipole interactions, lowers the energy of the emissive state and promotes a red shift. Only one study has attempted to interpret the three Gaussian components in spectroscopic and structural terms [57]. It is well established that the first emissive excited state of Laurdan type chromophores is a non-hydrogen bonded charge transfer state [51]. By comparing the emission maximum wavelength of the three Gaussian component to those of Laurdan in various solvents, Koehorst et al. [57] proposed that the three components correspond respectively in decreasing energy to (1) the non-hydrogen bonded charge transfer state, (2) a solvent hydrogen-bonded, solvent non-relaxed charge transfer state originating from (1), and (3) a solvent hydrogen-bonded, solvent-relaxed charge transfer state originating from (2). State (2) contributes the extra-component. For the probe in homogeneous fluid membranes, this component is absent or marginal due to significant water penetration and mobility that ensures complete or nearly complete conversion from state (2) to state (3) through dipolar relaxation. In more hindered and/or less hydrated environment, such conversion is incomplete and the extra-component can contribute largely to Laurdan emission spectra.

The Gaussian decomposition analysis of the steady-state Laurdan emission spectra in the whole temperature range studied (10 to 60 °C) was done for all LUV compositions studied. Fig. 5 presents some examples of this spectral decomposition for chosen temperatures for LUVs made of PC/SM/Chol 50:30:20 mol/mol. For 60 °C (Fig. 5A) and for 55 °C (data not shown), the emission spectra could be well analyzed as a composition of two Gaussian lines, centered as expected around 2.55 (486 nm) and 2.90 eV (430 nm). Below 55 °C, a two-Gaussian fit of the emission spectra leads to medium to low-quality results (examples on Fig. 5B and C, 40 and 20 °C respectively), becoming worse as the temperature decreases. On the other hand, the fluorescence spectra can be better-decomposed into three Gaussian line shapes. High-quality fits were obtained, as was judged by $\chi^2 > 0.99$ (Fig. 5D and E). As observed in others studies [57,62], the centers of the three Gaussian lines were found to vary around 2.58, 2.72 and 2.91 eV (480, 455, and 426 nm respectively) related to the energy level scheme of Laurdan. For pure L_o LUVs (SM/Chol 50:50 mol/mol), the analysis reveals that whatever the temperature between 10 and 60 °C, three Gaussian components are needed to obtain high-quality fits (Fig. S3, Supporting Information). This last feature also occurs after GM1 addition to the lipid mixture. For pure L_d LUVs (PC) and LUV composed of PC/GM1 90:10 mol/mol, three Gaussian components are only needed below 30 °C (Fig. S4, Supporting Information). Conclusions drawn from χ^2 values concerning the quality of two- and three-Gaussian fits were confirmed by residuals analyses which are plotted above each spectrum in Fig. 5.

Fig. 6 summarizes for all the bilayer compositions studied the Gaussian "extra-component" (~2.72 eV, i.e. ~ 455 nm) area fraction temperature dependence. Whatever the bilayer lipid composition, the Gaussian extra-component area fraction increases when the temperature decreases. The necessity of the extra-component in the fitting course is not simply related to mathematical fitting difficulties at high GP. This is borne out on the scatter plot of % extra-component vs. GP shown in Fig. S5 which shows that there is no unequivocal correlation between both parameters. Identical GP values may correspond to different % extra-component, depending on the lipid composition. Even for a single lipid composition, the % extra-component is not linearly related to the GP, the dependence being steeper at intermediate GP that at high or low GP. This suggests that the extra-component bears different information than the GP. Interestingly, there appears to be a significant correlation between the occurrence of the extra-component and the presence of a L_o phase. In Fig. 6, the points depicted in red are assumed to represent bilayers in the L_d phase, while those in blue symbolize bilayers with at least a fraction of the bilayer in the L_o phase. For LUVs made of PC/SM/Chol/GM1 50:30-*x*:20:*x* mol/mol, the T_{IP} values displayed in Fig. 4 have been used in order to determine the temperature threshold of L_o phase existence. One can see that the Gaussian extra-component per se can be considered as an index of the L_o phase above a threshold (red to blue symbol color change for a value of the extra-component area fraction around 0.09). As expected, the spectral decomposition in two or three Gaussian components reflects the temperature-dependent probe environment, and could be a way to detect L_o phase existence. Whereas the GP reports on the average order and packing of the bilayer, the % extra-component, above a minimal threshold, reports upon the bilayer phase heterogeneity, i.e. occurrence and amount of an ordered phase.

4. Discussion

In the present work, the effect of GM1 concentration on the L_o/L_d lateral phase separation in the PC/SM/Chol bilayers was studied. We showed that, in LUVs made of PC/SM/Chol/GM1 (50:30-*x*:20:*x* mol/mol), GM1 above 1 mol % abolishes the formation of the micrometer-scale L_o domains observed in GUVs for lower GM1 amounts (Fig. 1A). The

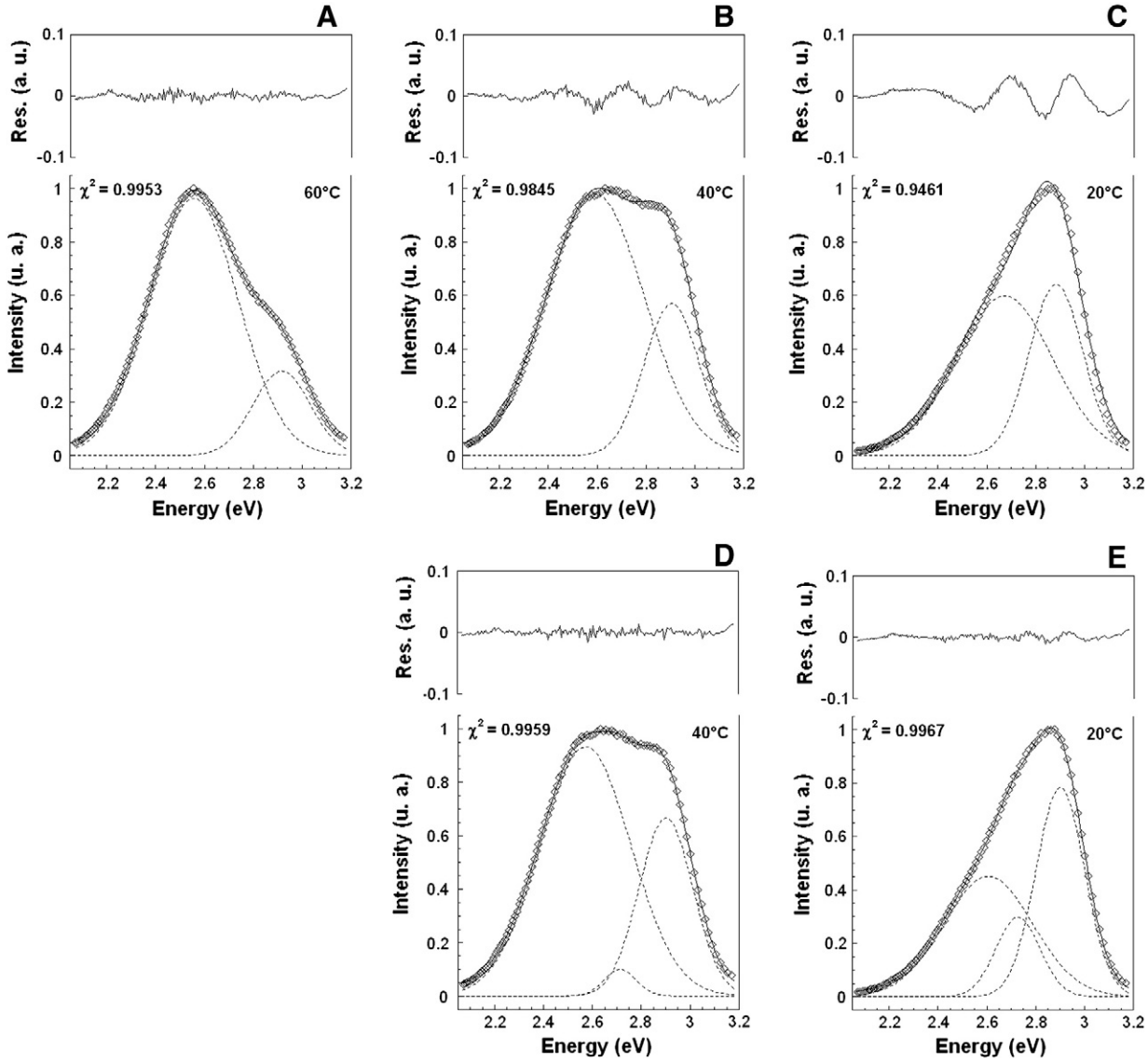

Fig. 5. Gaussian decomposition of fluorescence emission spectra of Laurdan in LUVs made of PC/SM/Chol 50:30:20 mol/mol at different temperatures. (A) 60 °C, two Gaussians; (B) 40 °C, two Gaussians; (C) 20 °C, two Gaussians; (D) 40 °C, three Gaussians; and (E) 20 °C, three Gaussians. The fitting of the experimental data (◊) was performed using IGOR 6.10A program using symmetrical Gaussians (dashed lines); solid lines are the sum of the different Gaussians. $\lambda_{exc} = 355$ nm. Residuals analyses are plotted above each spectrum.

homogeneous phase observed in optical microscopy corresponds in fact, for a certain temperature range, to a L_o/L_d lateral phase separation below the optical resolution. This nanoscale phase separation revealed by the self-quenching properties of C_{12}NBD-PC (Fig. 2) was supported by the Laurdan data (Figs. 3–6).

A question arose whether experiments with varying GM1 concentrations would yield different results if, instead of decreasing SM content in parallel with increasing GM1 content (as performed above), the 5:3:2 PC/SM/Chol molar ratio was kept constant while adding GM1. Control experiments were thus performed using the later approach. T_{IP} value changes from Laurdan experiments were below 0.6 °C for GM1 concentrations from 2 to 10% (Fig. S6 and Tab. S1). Such changes are of the same order of the experimental error. Therefore, although the question of the choice of the method is relevant, it does not seem to impact the data in the chosen GM1 concentration range.

Both NBD-PC and Laurdan GP measurements allowed us to determine the temperature range of formation of L_o phase domains over an L_d phase. At 0 mol % GM1 for example, the demixing temperature of phase separation determined by the self-quenching experiments is equal to 28.9 °C, close to the one (31.4 °C) defined by the position of the inflection point in the GP temperature dependence curve. The small difference can be explained by the distinct sensitivity to phase separation of the two measurements, and by the different probe effect on the bilayer organization in the two sets of experiments, as well as by fitting uncertainties. The inflection seen in the curves in Fig. 3A differs from the abrupt transition classically observed during gel–liquid disordered phase transition, and from the single concavity curve evolution of the GP in the course of gel–liquid ordered phase transition [63]. Consequently, we assume that the temperatures (T_{IP}, Fig. 4) determined at the inflection point of the temperature GP curves correspond approximately to the demixing temperature of L_o/L_d nanoscopic phase separation. Moreover, the T_{IP} values depend on the GM1 amount (x) in the PC/SM/Chol/GM1 (50:30-x:20:x) bilayers. The demixing temperatures of phase separation (Fig. 4) are shifted to higher values when x increases, which is linked with the change from SM to SM/GM1 of the dominant composition of L_o domains [39]. A possible explanation is that, in additional to the establishment of the stabilizing-lateral-segregation network of hydrogen bonds between ceramide moiety, lateral segregation of GM1 is further favored by the formation of hydrogen bonds between adjacent sugar residues [64].

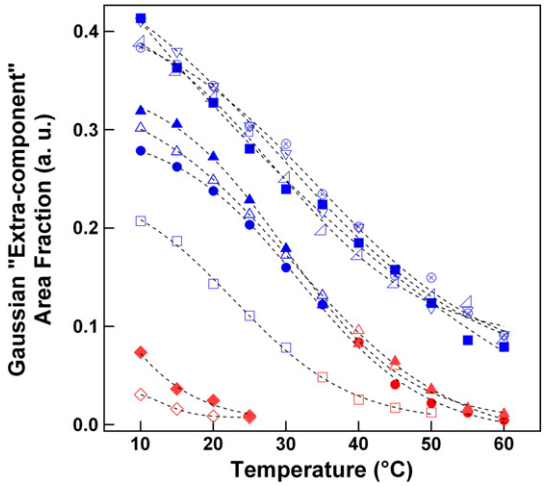

Fig. 6. Temperature dependence of the Gaussian extra-component area fraction. The area fraction is determined with the best fit of the Laurdan fluorescence spectra given by a three Gaussian decomposition analysis. For a specified lipid mixture, the absence of a point at a given temperature means that the spectrum has been better-decomposed in a two Gaussian line shapes. PC (◊); PC/GM1 90:10 (♦); PC/SM/Chol 50:30:20 (□ and □); PC/SM/Chol/GM1 50:30-*x*:20:*x* with $x = 1$ (● and ●), $x = 5$ (△ and △), and $x = 10$ (▲ and ▲); SM/Chol/GM1 with $x = 0$ (■), $x = 1$(⊗), $x = 5$ (◿), and $x = 10$ (▽). The points depicted in red are assumed to represent bilayers in the L_d phase, while those in blue symbolize bilayers with at least a fraction of the bilayer in the L_o phase.

These results were supported by the Laurdan spectra decomposition analysis showing that there is a significant correlation between the T_{IP} values and the temperature below which an extra-component becomes significant. Our proposal of the extra-component as an index of the L_o phase is consistent with the interpretation of Koehorst et al. [57] (see Section 3.4). Indeed the ordered nature of the L_o phase is characterized by a higher lipid packing density and therefore a lower available volume between lipid molecules. This likely corresponds to a lesser hydration and a lower lipid mobility of hydration water molecules and therefore a slower solvent relaxation around the Laurdan chromophore. To our knowledge, the mobility of water molecules bound to L_o phase bilayers has not been addressed yet. However, the study of M'Baye et al. [65] indeed shows that L_o phases have an intrinsic lower hydration than L_d phases. On the other hand, it does not seem that the extra-component is contributed by the environment located at the boundaries between L_o and L_d phases. Indeed, for each specific lipid composition, when the temperature is increased above T_{IP}, there is a L_o microdomain to L_o nanodomain transition which leads to an increase in the contribution of domain boundaries. However, such an increase of temperature promotes a decrease in the % extra-component (Fig. 6).

The fact that a small amount of extra-component is observable with L_d bilayers below 20 °C simply indicates that (2) → (3) dipolar relaxation at such low temperatures is slightly incomplete. This residual amount is 2–10% in our experiments.

Table 1 summarizes for the lipid mixtures designed to exhibit L_o/L_d phase coexistence, the values of the demixing temperature of L_o/L_d phase separation (T_{IP}) and the temperature of appearance of the micrometric L_o/L_d phase separation on GUVs ($T_{micro,}$ values derived from Fig. 1A). For the lipid mixtures known to exhibit this micrometric phase separation (0 and 1 mol % GM1), T_{IP} is greater than T_{micro} (there is no T_{micro} for mixtures with more than 1 mol % GM1). For example, at 0 mol % GM1, T_{IP} is equal to 31.4 °C and T_{micro} to 23 °C. In this framework, we propose that over the entire temperature range, the membrane at 0 mol % GM1 exhibits different morphologies or phases: (i) between 60.0 and 31.4 °C, the membrane is in a homogeneous L_d phase; (ii) at 31.4 °C, the nanoscale L_o/L_d phase separation occurs; and (iii) between 31.4 and 10 °C, the membrane exhibits a L_o/L_d phase coexistence but with discrete L_o microdomains observable over a continuous L_d phase only below 23 °C. A similar interpretation holds for the PC/SM/Chol bilayer containing 1 mol% GM1 (Table 1). There is therefore a range of L_o/L_d lipid mixtures (from 0 to 10 mol % GM1) that exhibit a L_o/L_d phase separation into nanodomains at specific but slightly different temperatures. Only a part of these mixtures (0 and 1 mol% GM1) undergo a L_o nano- to micro-domains transition when the temperature decreases. So, a new "morphological" phase diagram can be made (Fig. 7), which displays now three regions corresponding respectively to L_o/L_d micrometric phase separation (region I, Fig. 7), to L_o/L_d nanometric phase separation (region II, Fig. 7), and to a homogeneous L_d phase (region III, Fig. 7). Table 1 also indicates the range of % extra-component found by Gaussian analysis of Laurdan emission spectra between 10 °C, the lowest studied temperature and T_{IP}. There is a strong correlation between the increase of % extra-component at low temperature and the occurrence of a nanoscopic demixing transition. For L_d only bilayers (PC ± GM1), this component remains below 10% for this temperature range.

The analysis of the phase diagram displayed on Fig. 7 could be informative in different manners. 1) At a given temperature, one can see the effect of GM1 on the L_o/L_d phase separation. These composition-dependent data are particularly valuable, because composition is the primary mechanism by which a cell can alter membrane phase behavior. Around the physiological temperature for example, increasing GM1 content leads to a nanoscale L_o/L_d phase separation which is not present without GM1. Demixing temperature from L_d to L_o/L_d coexistence appears to be GM1 dependent. On the other hand, at 20 °C, the L_o/L_d phase coexistence always exists at least till 10 mol % GM1, but a threshold between micro- and nano-scale L_o/L_d phase separations occurs at 1 mol % GM1. Lipid composition alone can control the existence

Table 1
Effect of GM1 content on T_{IP}, T_{micro}, and on the Gaussian extra-component area fraction range between 10 °C and T_{IP} for vesicles composed of PC/SM/Chol/GM1 50:30-*x*:20:*x* mol/mol.

	GM1 content (mol %)[a]				
	0	1	2	5	10
T_{IP}[b]	31.4	34.9	35.4	36.9	38.2
T_{micro}[c]	23.0	20.0	None	None	None
Gaussian "extra-component" area fraction range between 10 °C and T_{IP}[d]	0.07-0.21	0.12-0.28	nd.	0.12-0.30	0.10-0.32

[a] GM1 content (*x* mol %) in PC/SM/Chol/GM1 (50:30-*x*:20:*x*) lipid systems.
[b] Temperature value at the inflection point for the curves displayed in Fig. 3A, following the procedure described in Fig. S1.
[c] Temperature of appearance of L_o microdomains over an L_d phase in GUVs (from Fig. 1A).
[d] Values extracted from Fig. 6.

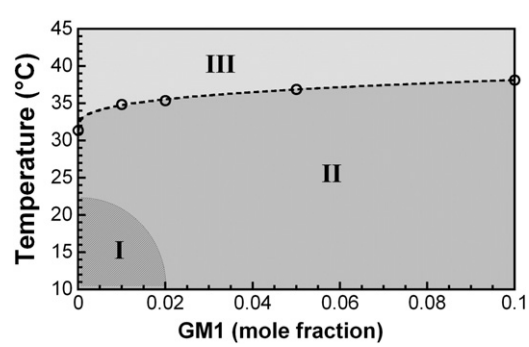

Fig. 7. GM1 content modulation of the L_o/L_d phase coexistence and the L_o domain size. Phase behavior of PC/SM/Chol/GM1 vesicles (GUVs and LUVs) as a function of temperature and GM1 mole fraction presented as a morphology diagram. Vesicles were prepared with the molar composition PC/SM/Chol/GM1 50:30-*x*:20:*x* ($0 \le x \le 10$) mol/mol. Each region represents one type of phase morphology: Region I, L_o microdomains over an L_d phase; region II, L_o nanodomains over an L_d phase; Region III, homogeneous L_d phase. The boundary between regions II and III is defined from the T_{IP} values (○) displayed on Fig. 4. The line is added only to guide the eye.

and the sizes of phase-separated membrane domains. This last feature seems characteristic of four-component lipid mixtures [32], while for three-component mixtures at constant temperature, depending on the lipid composition, the system exhibits one or the other domain size-scale (see for example Feigenson [19] in which notion of "type I" and "type II" mixtures is introduced, where the "type II mixtures" exhibit global phase separation, whereas the "type I mixtures" phase-separate on the nanoscale but are globally homogeneous, much like microemulsions). This naturally raises questions regarding the physical nature of the domain size modulation by GM1. A growing literature seeks to explain submicron domain stabilization in terms of composition-dependent membrane properties, like line tension, lipid–lipid dipolar repulsion, and curvature energies [66–68]. Indeed, the existence of two coexisting phases implies an energy associated with the interface between them. This energy per length, called line tension, is related to hydrophobic mismatch at domain boundaries and always favors coalescence of small domains into larger domains. Thermodynamic stability of small domains would require small line tension and a competing energy term favoring dispersed domains. A way to reduce line tension is the presence of line-active molecules, accumulating at the domain boundaries and bridging the differences in thickness. This role has been suggested for asymmetric saturated/monounsaturated lipids [69–71], but GM1, because of its saturated fatty acids (mainly palmitic and stearic acids) [72], seems not to fit such properties. However, as explained by Meinhardt et al. [67], an elastic tension, originating from a coupling between local composition and monolayer curvature, could be another source of a line tension decrease. The curvature mismatch between L_o and L_d phases is able to suppress global phase separation, and thereby stabilize submicron domains. In this framework, L_o-domain enriched GM1 with its cone-shape (GM1 shape factor around 0.5) appears as a good candidate for monolayer generating curvature, and this provides a convincing explanation of our experimental results. 2) At a given lipid composition, one can see the effect of temperature on the existing phases in the bilayer. While lipid mixtures with more than 1 mol % GM1 present only a nanoscale phase coexistence below the demixing temperature, lipid mixtures with 0 and 1 mol.% GM1 undergo a L_o nano- to micro-domain transition when the temperature decreases (Fig. 7 regions I and II). This could be explained by the increase of the line tension when the temperature decreases [18], favoring nanoscale domain coalescence, and leading ultimately to optically visible domains. Finally, with a marked dependence to local lipid composition and temperature, line tension appears to be of central importance for the phase-separation scale determination.

5. Conclusions

This work, carried out with four-component lipid model systems, investigates how lipid composition changes affect bilayer phase behavior. We show that GM1 content is able to modulate L_o/L_d phase coexistence and L_o domain size. Is it possible that this GM1 effect be a lipid-based mechanism of raft modulation in vivo? GM1 regulation in the plasma membrane is known to profoundly affect cell functions. For example, NEU3, described as plasma membrane ganglioside sialidase, has the ability to work on gangliosides that are located on the same membrane or on the membrane of adjacent cells, thus playing a central role in cell–cell interactions. NEU3 specifically localizes in lipid rafts. As a result of NEU3 activity, the cell content of gangliosides decreases, leading to a variation of the physicochemical properties of lipid rafts whose clustering represents a pivotal step for membrane fusion during myogenesis [73]. It has been also shown that the experimental overexpression of GM1 blocks PDGF receptor signaling by displacing it outside of lipid rafts [74], suggesting that local accumulation of GM1 might modulate receptor function. Finally, to try to answer the question at least partially, further investigations are needed, improving the model systems with the enzymatic conversion products of GM1. From a thermodynamic point of view, the role of GM1 on the line tension has to be clarified. In order to measure this possible dependence, we plan to analyze a set of L_o domain contours observed in GUV experiments (native domains for 0 and 1 mol % GM1, and photoinduced domains for higher concentration [47]) to extract the energies of the Fourier modes of domain fluctuations, and ultimately the values of the line tension corresponding to these modes [75,76].

Acknowledgments

This work was supported by grants from the CNRS (UMR7057), the Université Paris Diderot (19156), and the Bulgarian Fund for Scientific Research (DFNI-B01-5/2012). C. W. acknowledges the support of a Japan Student Services Organization (JASSO) fellowship. G. S. acknowledges the support of an invited professor grant from the Université Paris Diderot (Physics Department) during her stay in Paris.

Appendix A. Supplementary data

Supplementary data to this article can be found online at http://dx.doi.org/10.1016/j.bbamem.2014.05.002.

References

[1] A. Kusumi, K.G. Suzuki, R.S. Kasai, K. Ritchie, T.K. Fujiwara, Hierarchical mesoscale domain organization of the plasma membrane, Trends Biochem. Sci. 36 (2011) 604–615.
[2] R. Lindner, H.Y. Naim, Domains in biological membranes, Exp. Cell Res. 315 (2009) 2871–2878.
[3] D.A. Brown, E. London, Structure and function of sphingolipid- and cholesterol-rich membrane rafts, J. Biol. Chem. 275 (2000) 17221–17224.
[4] K. Simons, E. Ikonen, Functional rafts in cell membranes, Nature 387 (1997) 569–572.
[5] L.J. Pike, Rafts defined: a report on the Keystone Symposium on Lipid Rafts and Cell Function, J. Lipid Res. 47 (2006) 1597–1598.
[6] A. Pralle, P. Keller, E.L. Florin, K. Simons, J.K. Horber, Sphingolipid-cholesterol rafts diffuse as small entities in the plasma membrane of mammalian cells, J. Cell Biol. 148 (2000) 997–1008.
[7] K. Jacobson, O.G. Mouritsen, R.G. Anderson, Lipid rafts: at a crossroad between cell biology and physics, Nat. Cell Biol. 9 (2007) 7–14.
[8] D.A. Brown, E. London, Structure and origin of ordered lipid domains in biological membranes, J. Membr. Biol. 164 (1998) 103–114.
[9] C. Dietrich, L.A. Bagatolli, Z.N. Volovyk, N.L. Thompson, M. Levi, K. Jacobson, E. Gratton, Lipid rafts reconstituted in model membranes, Biophys. J. 80 (2001) 1417–1428.
[10] T. Harder, P. Scheiffele, P. Verkade, K. Simons, Lipid domain structure of the plasma membrane revealed by patching of membrane components, J. Cell Biol. 141 (1998) 929–942.
[11] P. Sengupta, B. Baird, D. Holowka, Lipid rafts, fluid/fluid phase separation, and their relevance to plasma membrane structure and function, Semin. Cell Dev. Biol. 18 (2007) 583–590.
[12] D. Lichtenberg, F.M. Goni, H. Heerklotz, Detergent-resistant membranes should not be identified with membrane rafts, Trends Biochem. Sci. 30 (2005) 430–436.
[13] H. Shogomori, D.A. Brown, Use of detergents to study membrane rafts: the good, the bad, and the ugly, Biol. Chem. 384 (2003) 1259–1263.
[14] A. Cambi, D.S. Lidke, Nanoscale membrane organization: where biochemistry meets advanced microscopy, ACS Chem. Biol. 7 (2012) 139–149.
[15] D.M. Owen, A. Magenau, D. Williamson, K. Gaus, The lipid raft hypothesis revisited—new insights on raft composition and function from super-resolution fluorescence microscopy, Bioessays 34 (2012) 739–747.
[16] J. Fan, M. Sammalkorpi, M. Haataja, Formation and regulation of lipid microdomains in cell membranes: theory, modeling, and speculation, FEBS Lett. 584 (2010) 1678–1684.
[17] D. Lingwood, K. Simons, Lipid rafts as a membrane-organizing principle, Science (New York, N.Y.) 327 (2010) 46–50.
[18] T. Baumgart, S.T. Hess, W.W. Webb, Imaging coexisting fluid domains in biomembrane models coupling curvature and line tension, Nature 425 (2003) 821–824.
[19] G.W. Feigenson, Phase diagrams and lipid domains in multicomponent lipid bilayer mixtures, Biochim. Biophys. Acta 1788 (2009) 47–52.
[20] S.L. Veatch, S.L. Keller, Seeing spots: complex phase behavior in simple membranes, Biochim. Biophys. Acta 1746 (2005) 172–185.
[21] K. Bacia, C.G. Schuette, N. Kahya, R. Jahn, P. Schwille, SNAREs prefer liquid-disordered over "raft" (liquid-ordered) domains when reconstituted into giant unilamellar vesicles, J. Biol. Chem. 279 (2004) 37951–37955.
[22] N. Puff, A. Lamaziere, M. Seigneuret, G. Trugnan, M.I. Angelova, HDLs induce raft domain vanishing in heterogeneous giant vesicles, Chem. Phys. Lipids 133 (2005) 195–202.
[23] G. Staneva, M.I. Angelova, K. Koumanov, Phospholipase A2 promotes raft budding and fission from giant liposomes, Chem. Phys. Lipids 129 (2004) 53–62.

[24] R.F. de Almeida, L.M. Loura, A. Fedorov, M. Prieto, Lipid rafts have different sizes depending on membrane composition: a time-resolved fluorescence resonance energy transfer study, J. Mol. Biol. 346 (2005) 1109–1120.
[25] M.L. Frazier, J.R. Wright, A. Pokorny, P.F. Almeida, Investigation of domain formation in sphingomyelin/cholesterol/POPC mixtures by fluorescence resonance energy transfer and Monte Carlo simulations, Biophys. J. 92 (2007) 2422–2433.
[26] F.A. Heberle, J. Wu, S.L. Goh, R.S. Petruzielo, G.W. Feigenson, Comparison of three ternary lipid bilayer mixtures: FRET and ESR reveal nanodomains, Biophys. J. 99 (2010) 3309–3318.
[27] G.W. Feigenson, J.T. Buboltz, Ternary phase diagram of dipalmitoyl-PC/dilauroyl-PC/cholesterol: nanoscopic domain formation driven by cholesterol, Biophys. J. 80 (2001) 2775–2788.
[28] T. Baumgart, A.T. Hammond, P. Sengupta, S.T. Hess, D.A. Holowka, B.A. Baird, W.W. Webb, Large-scale fluid/fluid phase separation of proteins and lipids in giant plasma membrane vesicles, Proc. Natl. Acad. Sci. 104 (2007) 3165–3170.
[29] I. Levental, M. Grzybek, K. Simons, Raft domains of variable properties and compositions in plasma membrane vesicles, Proc. Natl. Acad. Sci. U. S. A. 108 (2011) 11411–11416.
[30] J.F. Hancock, Lipid rafts: contentious only from simplistic standpoints, Nat. Rev. 7 (2006) 456–462.
[31] S.L. Goh, J.J. Amazon, G.W. Feigenson, Toward a better raft model: modulated phases in the four-component bilayer, DSPC/DOPC/POPC/CHOL, Biophys. J. 104 (2013) 853–862.
[32] T.M. Konyakhina, S.L. Goh, J. Amazon, F.A. Heberle, J. Wu, G.W. Feigenson, Control of a nanoscopic-to-macroscopic transition: modulated phases in four-component DSPC/DOPC/POPC/Chol giant unilamellar vesicles, Biophys. J. 101 (2011) L8–L10.
[33] B. Westerlund, J.P. Slotte, How the molecular features of glycosphingolipids affect domain formation in fluid membranes, Biochim. Biophys. Acta Biomembr. 1788 (2009) 194–201.
[34] S. Sonnino, A. Prinetti, Gangliosides as regulators of cell membrane organization and functions, Sphingolipids as Signaling and Regulatory Molecules, vol. 688, Springer, New York, 2010. 165–184.
[35] C. Reich, M.R. Horton, B. Krause, A.P. Gast, J.O. Radler, B. Nickel, Asymmetric structural features in single supported lipid bilayers containing cholesterol and GM1 resolved with synchrotron X-ray reflectivity, Biophys. J. 95 (2008) 657–668.
[36] M. Menke, S. Kunneke, A. Janshoff, Lateral organization of GM1 in phase-separated monolayers visualized by scanning force microscopy, Eur. Biophys. J. 31 (2002) 317–322.
[37] A. Radhakrishnan, T.G. Anderson, H.M. McConnell, Condensed complexes, rafts, and the chemical activity of cholesterol in membranes, Proc. Natl. Acad. Sci. 97 (2000) 12422–12427.
[38] C. Yuan, J. Furlong, P. Burgos, L.J. Johnston, The size of lipid rafts: an atomic force microscopy study of ganglioside GM1 domains in sphingomyelin/DOPC/cholesterol membranes, Biophys. J. 82 (2002) 2526–2535.
[39] R. Bao, L. Li, F. Qiu, Y. Yang, Atomic force microscopy study of ganglioside GM1 concentration effect on lateral phase separation of sphingomyelin/dioleoylphosphatidylcholine/cholesterol bilayers, J. Phys. Chem. B 115 (2011) 5923–5929.
[40] G. Staneva, A. Momchilova, C. Wolf, P.J. Quinn, K. Koumanov, Membrane microdomains: role of ceramides in the maintenance of their structure and functions, Biochim. Biophys. Acta 1788 (2009) 666–675.
[41] M.I. Angelova, D.S. Dimitrov, A mechanism of liposome electroformation, Prog. Collied Polym. Sci. 76 (1988) 59–67.
[42] G. Staneva, M. Seigneuret, K. Koumanov, G. Trugnan, M.I. Angelova, Detergents induce raft-like domains budding and fission from giant unilamellar heterogeneous vesicles: a direct microscopy observation, Chem. Phys. Lipids 136 (2005) 55–66.
[43] R.C. MacDonald, R.I. MacDonald, B.P.M. Menco, K. Takeshita, N.K. Subbarao, L.-R. Hu, Small-volume extrusion apparatus for preparation of large, unilamellar vesicles, Biochim. Biophys. Acta Biomembr. 1061 (1991) 297–303.
[44] N. Khalifat, J.B. Fournier, M.I. Angelova, N. Puff, Lipid packing variations induced by pH in cardiolipin-containing bilayers: the driving force for the cristae-like shape instability, Biochim. Biophys. Acta 1808 (2011) 2724–2733.
[45] V. Coste, N. Puff, D. Lockau, P.J. Quinn, M.I. Angelova, Ordering of lipid bilayer domains in large unilamellar vesicles probed by the fluorescent phospholipid analogue, C12NBD-PC, Biochim. Biophys. Acta Biomembr. 1758 (2006) 460–467.
[46] T. Parasassi, G. De Stasio, G. Ravagnan, R.M. Rusch, E. Gratton, Quantitation of lipid phases in phospholipid vesicles by the generalized polarization of Laurdan fluorescence, Biophys. J. 60 (1991) 179–189.
[47] G. Staneva, M. Seigneuret, H. Conjeaud, N. Puff, M.I. Angelova, Making a tool of an artifact: the application of photoinduced L_o domains in giant unilamellar vesicles to the study of L_o/L_d phase spinodal decomposition and its modulation by the ganglioside GM1, Langmuir 27 (2011) 15074–15082.
[48] A. Ferraretto, M. Pitto, P. Palestini, M. Masserini, Lipid domains in the membrane: thermotropic properties of sphingomyelin vesicles containing GM1 ganglioside and cholesterol, Biochemistry 36 (1997) 9232–9236.
[49] A. Chattopadhyay, E. London, Spectroscopic and ionization properties of N-(7-nitrobenz-2-oxa-1,3-diazol-4-yl)-labeled lipids in model membranes, Biochim. Biophys. Acta Biomembr. 938 (1988) 24–34.
[50] S. Mazeres, V. Schram, J. Tocanne, A. Lopez, 7-Nitrobenz-2-oxa-1,3-diazole-4-yl-labeled phospholipids in lipid membranes: differences in fluorescence behavior, Biophys. J. 71 (1996) 327–335.
[51] R.S. Brown, J.D. Brennan, U.J. Krull, Self-quenching of nitrobenzoxadiazole labeled phospholipids in lipid membranes, J. Chem. Phys. 100 (1994) 6019–6027.
[52] D. Hoekstra, Fluorescence method for measuring the kinetics of Ca^{2+}-induced phase separations in phosphatidylserine-containing lipid vesicles, Biochemistry 21 (1982) 1055–1061.
[53] R.M.R.S. Mesquita, E. Melo, T.E. Thompson, W.L.C. Vaz, Partitioning of amphiphiles between coexisting ordered and disordered phases in two-phase lipid bilayer membranes, Biophys. J. 78 (2000) 3019–3025.
[54] R. Koynova, M. Caffrey, Phases and phase transitions of the phosphatidylcholines, Biochim. Biophys. Acta 1376 (1998) 91–145.
[55] L. Bagatolli, E. Gratton, Direct observation of lipid domains in free-standing bilayers using two-photon excitation fluorescence microscopy, J. Fluoresc. 11 (2001) 141–160.
[56] P.F. Almeida, W.L. Vaz, Lateral diffusion in membranes, in: R. Lipowsky, E. Sackmann (Eds.), Structure and Dynamics of Membranes, vol. 1A, Elsevier, 1995, pp. 305–357.
[57] R.B.M. Koehorst, R.B. Spruijt, M.A. Hemminga, Site-directed fluorescence labeling of a membrane protein with BADAN: probing protein topology and local environment, Biophys. J. 94 (2008) 3945–3955.
[58] S.L. Frey, E.Y. Chi, C. Arratia, J. Majewski, K. Kjaer, K.Y. Lee, Condensing and fluidizing effects of ganglioside GM1 on phospholipid films, Biophys. J. 94 (2008) 3047–3064.
[59] L. Mainali, M. Raguz, W.K. Subczynski, Phase-separation and domain-formation in cholesterol-sphingomyelin mixture: pulse-EPR oxygen probing, Biophys. J. 101 (2011) 837–846.
[60] A. Lúcio, C. Vequi-Suplicy, R. Fernandez, M. Lamy, Laurdan spectrum decomposition as a tool for the analysis of surface bilayer structure and polarity: a study with DMPG, peptides and cholesterol, J. Fluoresc. 20 (2010) 473–482.
[61] D. Ionescu, C. Ganea, A study of quercetin effects on phospholipid membranes containing cholesterol using Laurdan fluorescence, Eur. Biophys. J. 41 (2012) 307–318.
[62] S. Vanounou, D. Pines, E. Pines, A.H. Parola, I. Fishov, Coexistence of domains with distinct order and polarity in fluid bacterial membranes, Photochem. Photobiol. 76 (2002) 1–11.
[63] F.M. Harris, K.B. Best, J.D. Bell, Use of laurdan fluorescence intensity and polarization to distinguish between changes in membrane fluidity and phospholipid order, Biochim. Biophys. Acta Biomembr. 1565 (2002) 123–128.
[64] E. Posse de Chaves, S. Sipione, Sphingolipids and gangliosides of the nervous system in membrane function and dysfunction, FEBS Lett. 584 (2010) 1748–1759.
[65] G. M'Baye, Y. Mely, G. Duportail, A.S. Klymchenko, Liquid ordered and gel phases of lipid bilayers: fluorescent probes reveal close fluidity but different hydration, Biophys. J. 95 (2008) 1217–1225.
[66] D.W. Lee, Y. Min, P. Dhar, A. Ramachandran, J.N. Israelachvili, J.A. Zasadzinski, Relating domain size distribution to line tension and molecular dipole density in model cytoplasmic myelin lipid monolayers, Proc. Natl. Acad. Sci. U. S. A. 108 (2011) 9425–9430.
[67] S. Meinhardt, R.L.C. Vink, F. Schmid, Monolayer curvature stabilizes nanoscale raft domains in mixed lipid bilayers, Proc. Natl. Acad. Sci. 110 (2013) 4476–4481.
[68] M. Schick, Membrane heterogeneity: manifestation of a curvature-induced microemulsion, Phys. Rev. E. 85 (2012) 031902.
[69] R. Brewster, S.A. Safran, Line active hybrid lipids determine domain size in phase separation of saturated and unsaturated lipids, Biophys. J. 98 (2010) L21–L23.
[70] L.V. Schafer, S.J. Marrink, Partitioning of lipids at domain boundaries in model membranes, Biophys. J. 99 (2010) L91–L93.
[71] O. Szekely, Y. Schilt, A. Steiner, U. Raviv, Regulating the size and stabilization of lipid raft-like domains and using calcium ions as their probe, Langmuir 27 (2011) 14767–14775.
[72] S. Sonnino, L. Mauri, V. Chigorno, A. Prinetti, Gangliosides as components of lipid membrane domains, Glycobiology 17 (2006) 1R–13R.
[73] A. Fanzani, A. Zanola, F. Faggi, N. Papini, B. Venerando, G. Tettamanti, M. Sampaolesi, E. Monti, Implications for the mammalian sialidases in the physiopathology of skeletal muscle, Skelet. Muscle 2 (2012) 23.
[74] T. Mitsuda, K. Furukawa, S. Fukumoto, H. Miyazaki, T. Urano, K. Furukawa, Overexpression of ganglioside GM1 results in the dispersion of platelet-derived growth factor receptor from glycolipid-enriched microdomains and in the suppression of cell growth signals, J. Biol. Chem. 277 (2002) 11239–11246.
[75] J. Ehrig, E.P. Petrov, P. Schwille, Phase separation and near-critical fluctuations in two-component lipid membranes: Monte Carlo simulations on experimentally relevant scales, New J. Phys. 13 (2011).
[76] C. Esposito, A. Tian, S. Melamed, C. Johnson, S.Y. Tee, T. Baumgart, Flicker spectroscopy of thermal lipid bilayer domain boundary fluctuations, Biophys. J. 93 (2007) 3169–3181.